



*Research article*

## **The effect of RAP content on fatigue damage property of hot reclaimed asphalt mixtures**

**Longting Ding<sup>1</sup>, Yuan Li<sup>2,\*</sup>, Zhanchuang Han<sup>3</sup>, Mengyuan Zhang<sup>1,\*</sup>, Xuancang Wang<sup>2</sup> and Lu He<sup>4</sup>**

<sup>1</sup> Innovation Research Institute, Shandong Hi-speed Group Co., Ltd, Jinan 250001, China

<sup>2</sup> Key Laboratory for Special Area Highway Engineering of Ministry of Education, Chang'an University, Xi'an 710064, China

<sup>3</sup> CCCC First Highway Engineering Group Co., Ltd, Beijing 100024, China

<sup>4</sup> Jinan Urban Construction Group, Jinan 250001, China

\* **Correspondence:** Email: [liyuan\\_mm@chd.edu.cn](mailto:liyuan_mm@chd.edu.cn), [zmyy2018@163.com](mailto:zmyy2018@163.com).

**Abstract:** The fatigue property of the recycled mixture affects the structural design of recycled pavement. In order to explore the effect of different reclaimed asphalt pavement (RAP) content on the fatigue properties of recycled mixtures, the fatigue properties of recycled mixtures were analyzed through an indoor fatigue test and finite element numerical simulation. Based on the phenomenological method and the dissipated energy theory, the fatigue properties of recycled mixtures with different RAP contents were analyzed and the fatigue damage of the mixtures were also studied under various strain levels. Based on the finite element numerical model of fatigue damage, the stress distribution and internal damage field distribution of trabecular specimens under different temperatures, strain levels and RAP contents were analyzed. The results showed that the anti-fatigue level of the mixture decreased as the RAP content was increased. The relative change rate of dissipated energy for different types of mixtures showed a two-stage change rule with the change of load times, that is, the value is large and decreasing, and the value is small and stable. The correlation between the plateau value (PV) and the fatigue life was established under the double logarithm coordinates, which could better analyze the influence law of the RAP content on the fatigue performance of the recycled mixture. Under different temperatures, strain levels, and RAP contents, the stress at the bottom of trabecular specimen and the overall damage field were mainly generated at the upper part under compressive stress and the bottom under tensile stress, and the damage field distribution area accounted for a small part of the whole specimen. According to the test results and fatigue damage distribution, it is recommended that the

content of recycled aggregate in recycled asphalt mixtures be less than 30% to ensure good performance. The research results have important practical significance for the improvement of fatigue performance and engineering application of recycled mixtures.

**Keywords:** road engineering; recycled mixture; mechanical damage calculation; RAP content; fatigue performance; fatigue damage

---

## 1. Introduction

Fatigue damage caused by repeated loading is one of the main problems affecting the long-term road performance of the mixture. As it is affected by many factors such as temperature, frequency, and load level, the research on fatigue performance of recycled mixtures has become the focus of many scholars.

At present, studies on the fatigue of mixtures are mainly divided into phenomenological methods, fracture mechanics methods, energy methods, and viscoelastic continuous damage mechanics methods [1]. Heveem et al. [2] was the first to study pavement fatigue life and establish the relationship between the fatigue life and tensile strain of asphalt pavement bottom. Pell et al. [3] proposed a fatigue life prediction model considering the power function-controlled strain conditions. Monismith et al. [4] proposed a fatigue life prediction model considering stiffness modulus. Academician Zheng [5] proposed a viscoelastic damage evolution model for asphalt mixture and established a nonlinear fatigue damage theory by analyzing the relationship between fatigue under stress and strain modes. Lv [6] proposed a viscoelastic fatigue damage model combined with the Burgers model and obtained the model parameters. Ge et al. [7] established the normalized fatigue characteristic model of asphalt mixtures through the strength and fatigue test, and proposed to use the normalized model to describe the fatigue characteristic of asphalt mixtures at various temperatures and stress levels. Sudarsanan et al. [8] analyzed the most used phenomenological models and mechanical models for predicting the fatigue life of asphalt pavement, and concluded that the two main defects of the commonly used fatigue life prediction models for pavement structures are the sensitivity of experimental results and the lack of reliability of some predictive models. In addition, they proposed multi-scale asphalt material characterization as an ongoing practice to determine the most appropriate performance evaluation tool.

Tapsobaa et al. [9] conducted fatigue tests and proposed that a recycled asphalt pavement (RAP) content of 40% could significantly improve the fatigue performance of a regenerated mixture. Monismith et al. [10] proposed that adding the biomodified binder to the recycled mixture with high RAP content could improve its fatigue characteristics. Visintine and Kavussi et al. [11,12] proposed that the fatigue life of the reclaimed asphalt mixture was greatly related to percent of recycled material it contained and the initial assumed stress level. Schuster et al. [13] tested the fatigue properties of 24 asphalt mixtures by using the 2S2P1D rheological model (two springs, two parabolic elements, and one dashpot) and the simplified viscoelastic continuum damage (S-VECD) model, and they concluded that the fatigue properties of the mixtures had nothing to do with viscoelastic linear behavior. Huang et al. [14,15] carried out trabecular bending fatigue tests on recycled mixtures with different RAP contents, and they concluded that with the increase of RAP content, the fatigue resistance gradually decreased. And the permissible tensile strain was obtained by modifying the fatigue equation with power function. Tan et al. [16] conducted four-point bending fatigue tests on hot mix, warm recycled

mixtures, and hot recycled mixtures. It was concluded that the fatigue performance of warm recycled mix was better than that of hot recycled mix, but lower than that of hot mix asphalt, and the difference was more obvious at high strain levels. He et al. [17] conducted a fatigue test on AC-13 and AC-16 recycled mixtures using a universal material testing machine and determined that the fatigue properties and sensitivity to stress of mixtures gradually declined with the increase of RAP content. Wang et al. [18] designed three structural combinations of hot mix and cold recycled mix with different thicknesses, studied the fatigue properties of the three composite structures through fatigue tests, and used an artificial neural network to predict the fatigue life of each composite structure to determine the optimal combination. Noura et al. [19] studied the fatigue and stiffness characteristics of asphalt mixtures made of different types of recycled aggregates, and the test results showed that compared with conventional mixtures, recycled asphalt mixtures had superior stiffness characteristics and improved fatigue life. In addition, the existing fatigue life prediction model of mixtures was optimized in the study. Sapkota et al. [20] studied the application of recycled aggregate asphalt mixtures in roads with light to medium traffic. They increased the proportion of recycled aggregates in hot mix asphalt to 100%, and the results showed that the mixture with 100% recycled aggregate had superior mechanical and resilient modulus performances.

In summary, the current research on the fatigue properties of recycled asphalt mixtures mainly focuses on performance evaluation of different influencing factors, analysis of test methods and life prediction, etc. In the aspect of life prediction, performance evaluation models such as the fatigue life prediction model and fatigue damage model are established. Based on laboratory tests and simulation, this paper studied the fatigue damage properties and fatigue damage field distribution of recycled mixtures. Based on the phenomenological method and dissipated energy theory, the fatigue property variation and fatigue damage of recycled mixtures with different RAP contents were analyzed. Furthermore the stress distribution at the bottom of trabecular specimens and the internal damage field distribution under different temperatures, strain levels and RAP contents were obtained in order to explore the fatigue properties of the recycled mixtures and provide references for engineering practice.

## 2. Materials and mixture gradation

### 2.1. Material properties

#### 2.1.1. Asphalt

The asphalt used was 90# matrix asphalt, and its performance indexes are shown in Table 1.

**Table 1.** Performance indices of 90# matrix asphalt.

Test indices	Test result	Standard [21]
Penetration (25 °C, 5 s, 100 g) (0.1 mm)	85.2	80–100
15 °C Ductility (cm)	105.6	≥ 100
Softening point (°C)	46	≥ 45
Penetration ratio (%)	68.9	≥ 57
RTFOT 10°C Ductility (cm)	38.7	≥ 8
Mass loss (%)	-0.02	≤ ± 0.8

### 2.1.2. Aggregate and mineral powder

The indexes of RAP material were tested, and the performance met the requirements. The test results are shown in Table 2. New aggregate should be added to the recycled mixture, and the test results are shown in Table 3.

**Table 2.** Test results of recycled aggregate.

Aggregate	Test index	Test result	Standard [21]
Coarse aggregate	Needle flake content (%)	8.6	Measured
	Crushing value (%)	20.8	$\leq 28$
	Angular (flow time, s)	26.4	Measured
Fine aggregate	Needle flake content (%)	11.2	Measured
	Crushing value (%)	21.8	Surface layer $\leq 26$ other $\leq 28$
	Sand equivalent (%)	65	$\geq 60$

**Table 3.** Test results of coarse aggregate.

Test indices	Test result	Standard [21]
Crushing value (%)	19	$\leq 28$
Needle flake content (%)	8.0	$\leq 18$
Particle content (%)	0.3	$\leq 1$
Adhesion to asphalt	4.5	$\geq 4$

The mineral powder was produced in Inner Mongolia, China, and the test results [22] are shown in Table 4.

**Table 4.** Test results of mineral powder.

Test indices (Granularity range)	Test result	Standard (Expressways) [21]
< 0.6 mm	100	100
< 0.15 mm	99.9	90–100
< 0.075 mm	89.4	75–100
Appearance	No clumping	No clumping

### 2.1.3. Rejuvenator

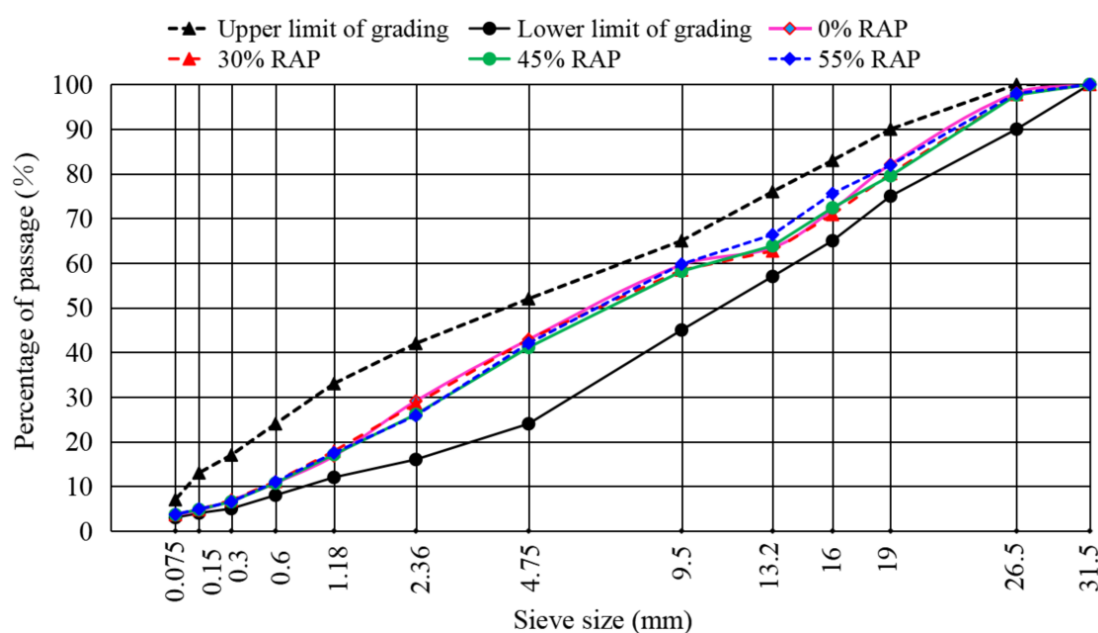
The rejuvenator was type A rejuvenator produced by a company in China, and its performance indexes are shown in Table 5.

**Table 5.** Performance indexes of type A rejuvenator.

Test indexes	Test results	Standard	Test method [23]
Viscosity, 60 °C, cSt	2860	actual	T0619
Flash point, °C	226	$\geq 220$	T0633
Saturation content, %	23	$\leq 30$	T0618
Aromatic content, %	39.8	actual	T0618
15 °C relative density	0.986 (liquid state)	actual	T0603
RTFOT	Viscosity ratio	$\leq 3$	T0619
	Mass loss, %	$\pm 3$	T0609

## 2.2. Recycled mixture gradation design

The gradation of recycled mixture should meet the relevant requirements of JTG F40 [21]. The dosages of RAP were 0, 30, 45 and 55%. Considering the application of recycled mixtures to the underlayer of pavement, the design grading was determined according to the grading range of AC-25 in the specification. The gradation design of mixed materials with different dosages of RAP was carried out respectively, and the final gradation was determined in Figure 1.

**Figure 1.** Grading diagram of recycled mixture.

The optimum rejuvenator content was determined to be 8% (old asphalt in RAP) by blending method. According to JTG/T 5521[24], the amount of new asphalt (P) in the recycled mixture with different dosages of RAP was calculated. Then, the Marshall test was carried out with five asphalt dosages of P,  $P \pm 0.5$ , and  $P \pm 1.0$  to determine the optimal amount of asphalt in hot recycled mixture with different dosage of RAP (excluding the old asphalt in RAP). Finally the gradation of AC-25 hot recycled mixture was obtained, as shown in Table 6.

**Table 6.** Gradation design of RAP regenerated mixture with different admixtures.

RAP dosage	RAP (mm)			New material (mm)			Mineral powder	Binder-aggregate ratio	
	10~30	5~10	0~5	20~30	10~20	5~10			0~5
0%	0	0	0	16	27	18	36	3	4.5
30%	4	16	10	19	22	0	26	3	3.58
45%	14	15	16	20	14	0	18	3	3.45
55%	19	14	22	17	12	0	13	3	3.12

### 3. Results

#### 3.1. Indoor fatigue test design

Fatigue tests were carried out by T0739 method in JTG E20 [23] to study the fatigue property of recycled asphalt mixtures. Compared with the traditional wheel rolling molding, the shear compactor (ASC) molding could effectively simulate the shear effect and compaction state of the mixture under actual pressure, and achieve the same voidage as the actual road condition, providing good consistency and reproducibility for the simulation of actual road fatigue. A shear compactor was used in the test to form the specimen (cuboid test block  $450 \times 150 \times 180$  mm) by inputting the density and height of the recycled mixture. After demolding, standard trabecular specimens with a length of  $380 \pm 5$  mm, width of  $63.5 \pm 5$  mm, and thickness of  $50 \pm 5$  mm were cut. The specimen forming process is shown in Figure 2.



**Figure 2.** Forming and cutting of specimen.

UTM-100 and a pneumatic four-point bending fatigue testing machine were selected for fatigue tests, and the process is shown in Figure 3. In order to simulate the stress state of the pavement under actual load, the 10 Hz loading frequency was selected, and the loading waveform of partial sine wave was adopted during the test. When the bending stiffness modulus drops to 50% of the initial stiffness modulus, the corresponding fatigue frequency was recorded as the fatigue life of the mixture. The

strain control was adopted, and the strain levels were determined to be  $400 \mu\epsilon$ ,  $500 \mu\epsilon$  and  $600 \mu\epsilon$  through the test.

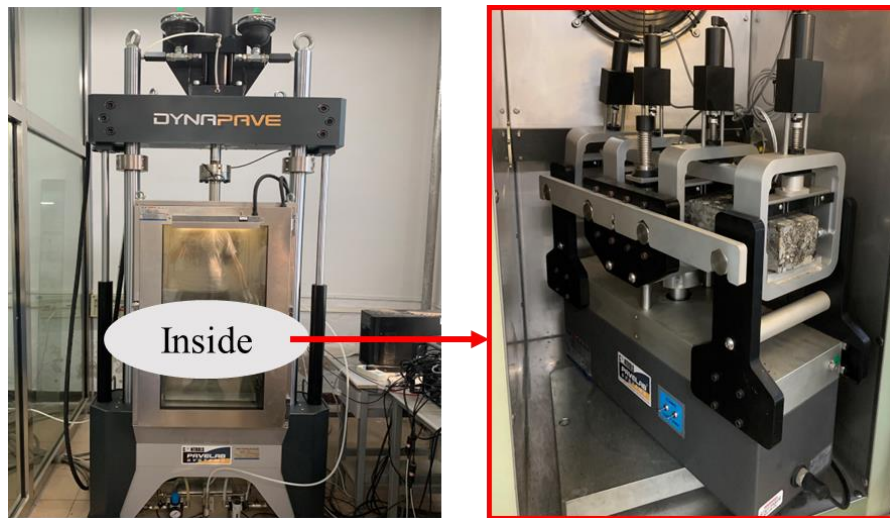


**Figure 3.** Four-point bending fatigue test.

According to the above test conditions and parameter selection, the regeneration specimens with different RAP content were formed according to the determined gradation and asphalt dosage, and then the fatigue performance tests were carried out.

### 3.2. Phenomenological analysis

Many scholars have established a large number of models to evaluate the fatigue performance of asphalt mixtures. The commonly-used prediction models of asphalt mixture fatigue used by Chinese scholars include models with tensile strain, asphalt saturation, and dynamic modulus as parameters proposed by South China University of Technology, and the fatigue life prediction equation recommended in asphalt pavement design specifications [25]. In addition, the commonly-used models [26] include the Westrack model, SHELL model, and SHRP equation. Among them, the most classic model is the strain based fatigue prediction equation proposed by Pell of Nottingham University [27], as shown in Eq (1).

$$N_f = c * (1 / \epsilon)^b \quad (1)$$

where  $N_f$  is the frequency of fatigue action,  $\epsilon$  the strain level,  $b$  and  $c$  are fitting parameters.

Take the logarithm of both sides of the above equation to get Eq (2).

$$\log N_f = \log c - b \log \epsilon = a - b \log \epsilon \quad (2)$$

In the double logarithm coordinates above, slope  $b$  of the fatigue equation could be used to reflect

the sensitivity between fatigue life and load strain of asphalt mixture, and the greater the value, the greater the sensitivity. Intercept  $a$  represented the fatigue life of asphalt mixture at low strain level, and the larger the value, the better the anti-fatigue level of asphalt mixture [28].

### 3.3. Energy analysis

Asphalt mixtures are a kind of viscoelastic-plastic material. In order to cope with the action of external load, the structure would change to adapt to the load condition. This change is essentially a process of energy consumption, and energy consumption generated in response to load is dissipated energy [29].

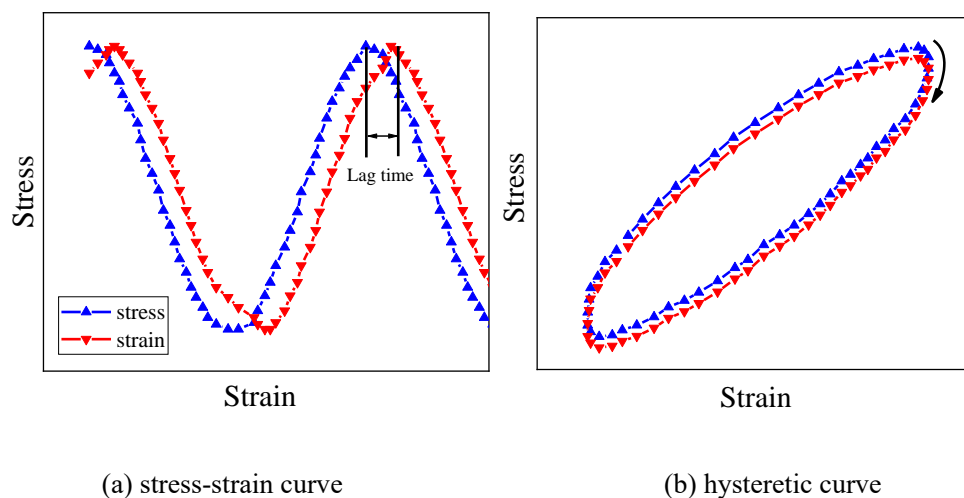


**Figure 4.** Stress-strain lag time and curve.

Many scholars have proposed to study the fatigue characteristics of asphalt mixture from the aspect of dissipated energy theory. The stress-strain lag time and hysteresis curve are shown in Figure 4. There would be a certain lag in the stress-strain response of materials under load. The phase angle of viscoelastic materials could be obtained from the lag time by Eq (3). The annular area of an approximate ellipse enclosed by a hysteresis curve in one period is the dissipated energy in one period. When the strain amplitude was unchanged, the stress of the specimen would decrease with the increase of the number of cycles, the hysteresis curve would gradually move, the closed area would decrease, and the dissipative energy would decrease.

$$\varphi = 360f \cdot t \quad (3)$$

where  $f$  is the loading frequency ( $Hz$ ),  $t$  is the time when the strain peak lags behind the stress peak ( $s$ ).

According to the research of relevant domestic scholars [30], the ratio of dissipated energy change (RDEC) is reliable for analyzing the fatigue properties of asphalt mixtures. Therefore, RDEC is used to characterize the damage degree of various regenerated mixtures. The equation of RDEC is as follows:

$$RDEC = |DE_{i+1} - DE_i| / DE_i \quad (4)$$



where  $DE_{i+1}$  is the dissipated energy of the  $i+1$ st time,  $DE_i$  is the dissipated energy of the  $i$ th time.

Since the number of cycles of the experimental data was 10, the equation was transformed to facilitate calculation. RDEC with equal interval was obtained as the fatigue evaluation index, as shown in Eq (5).

$$RDEC = |DE_j - DE_i| / DE_i(j-i) \quad (5)$$

where  $DE_j$  is the dissipated energy of the  $j$ th time,  $DE_i$  is the dissipated energy of the  $i$ th time.

Therefore, RDEC could be used to evaluate the fatigue properties of different recycled asphalt mixtures. The relative change rates of dissipated energy of the recycled asphalt mixtures with different RAP contents under different strain levels were calculated respectively.

#### 3.4. Fatigue damage variables analysis

Fatigue damage [31] refers to the process of unrecoverable strength attenuation and accumulation of materials under repeated loads. The damage process is often accompanied by changes in the properties of materials, such as changes in material strength and modulus. Therefore, the change of physical parameters such as dissipated energy and stiffness modulus could be used to characterize the damage magnitude of materials. It is difficult to calculate fatigue damage by theoretical calculation, so it focuses on studying the attenuation of physical and mechanical properties of materials under repeated loads. When applying damage mechanics to solve fatigue damage, it is necessary to determine how to measure fatigue damage. The damage variable is initially defined as the reduction of the effective bearing cross-sectional area of the material under load. That is:

$$D = \frac{A - A^*}{A} = 1 - \frac{A^*}{A} \quad (6)$$

where  $D$  is the material damage rate,  $A^*$  is the effective bearing area, and  $A$  is the carrying capacity in the non-destructive state.

Although the equation is simple to understand, it is very difficult to obtain the variation of the bearing area of the material. The researchers looked for parameters that could be measured directly or calculated indirectly to express fatigue damage. Lemaitre et al. [32] proposed the strain equivalent hypothesis theory. The deformation of materials due to stress was equivalent to the deformation of virtual lossless materials, and the effective bearing area of damaged materials and virtual lossless materials was equal. Similarly, relevant scholars [33] put forward the hypothesis of strain equivalence, used the relation of nondestructive materials to characterize the constitutive relation of damaged materials, and used  $\varepsilon^*$  to represent the effective strain, as shown in Eq (7).

$$\varepsilon^* = \varepsilon \times (1 - D) \quad (7)$$

The test was carried out under strain control mode, that is, when repeated loads were applied each time, the strain level remained unchanged and the stress decreased with the action of repeated loads.

Under  $n$  loads, the material's modulus  $S_n$  can be expressed as:

$$S_n = \sigma_t(n) / \varepsilon_t \quad (8)$$

The stiffness modulus of the material in its initial state could be expressed as:

$$S_0 = \sigma_t / \varepsilon_t \quad (9)$$

Based on the stress-strain equivalent hypothesis theory, the relationship after material damage could be expressed as:

$$S_0 = \sigma_t(n) / \varepsilon_t^* = \sigma_t(n) / (\varepsilon_t \times (1 - D)) \quad (10)$$

Substitute Eq (8) into Eq (10):

$$S_0 = S_n / (1 - D) \quad (11)$$

Then, the fatigue damage variable  $D$  expressed by bending stiffness modulus could be obtained as follows:

$$D = 1 - \frac{S_n}{S_0} \quad (12)$$

Combined with fatigue test data, the equation could be used to calculate the fatigue damage variables of each regenerated mixture under different test conditions by using the test results of the bending stiffness modulus. Then, it would be possible to evaluate the influence of different strain levels and influencing factors on the fatigue damage of the regenerated mixture.

### 3.5. Finite element analysis model

ABAQUS 2018 finite element software was used to build the trabecular model, and the tensile stress and internal damage of the specimens were calculated and analyzed. The trabecular model was set to  $380 \text{ mm} \times 63.5 \text{ mm} \times 50 \text{ mm}$  according to the actual specimen size. In order to simulate the actual loading process, four sets of fixed fixtures were set to fix and load the trabecular specimen. The width of the fixture was 25 mm, the thickness was 1 mm, and the distance between the center point of the adjacent fixture was about 119 mm. The upper and lower sides of the specimen and fixture were set as frictional contact while the lateral contact was frictionless. The vertical and horizontal displacements were restricted at the two lateral supports, but the rotation was not restricted. The horizontal and lateral displacement of the inner two clamps were restrained, and the vertical displacement was not restrained. The vertical displacement load was applied to simulate the loading process. The dead weight of the specimen was not considered in the modeling. The specimen was assumed to be a homogeneous linear elastic body, and the element type was three-dimensional eight-node structural element (C3D8). After the finite element model was established according to the actual trabecular specimen, and the model is mesh-divided by the specification grid planning method. The

mesh size was 6 mm, the model as shown in Figure 5. The mixtures with different RAP contents in the model were realized by setting different dynamic modulus, which were obtained through laboratory tests at 20 °C and 10 Hz.

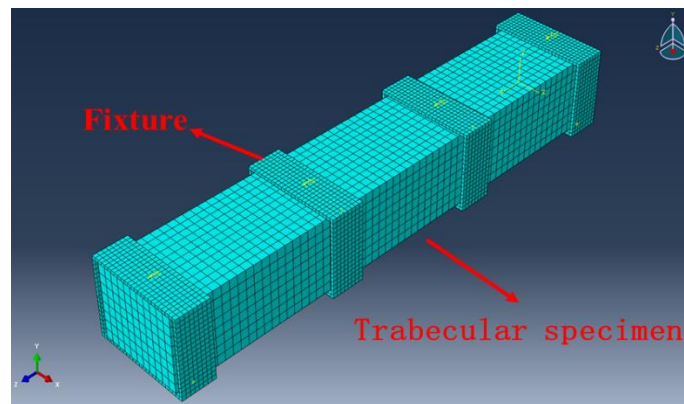


**Figure 5.** Trabecular specimen model.

Based on the damage theory, combined with the static equation, physical equation, and geometric equation of trabecular specimen under stress, the damage field distribution inside the trabecular was deduced. In this paper, the fatigue damage of recycled asphalt mixtures under different influencing factors was analyzed by referring to the asphalt mixture fatigue damage constitutive model of related researchers [34,35].

## 4. Results and discussion

### 4.1. Fatigue performance analysis based on phenomenology analysis

The fatigue test results of recycled mixtures with different RAP content are shown in Table 7.

**Table 7.** Fatigue test results of recycled mixture.

RAP content	Strain level ( $\mu\epsilon$ )	Initial stiffness modulus (MPa)	Fatigue life (time)	Average phase angle ( $^{\circ}$ )	Cumulative dissipated energy ( $\text{MJ/m}^3$ )
0%	400	10,419.2	69,010	44.1	153.7
	500	10,791.7	19,000	45.5	69
	600	8955.9	11,200	47.4	48.2
30%	400	13,510.9	63,050	38.1	171.7
	500	12,509.1	16,010	43.7	68.6
	600	9930.8	10,790	47.9	53.6
45%	400	10,217.4	35,480	48.9	76.2
	500	10,236.8	9030	51.4	31.9
	600	8069.4	6220	54.5	25.2
55%	400	8624.1	26,130	46	52.1
	500	10,890.7	8400	57.4	31.4
	600	9260.4	5110	57.5	23.7

Fatigue Eq (2) was used to fit the test results in Table 7 with double logarithm, and the fitting results were shown in Figure 6.

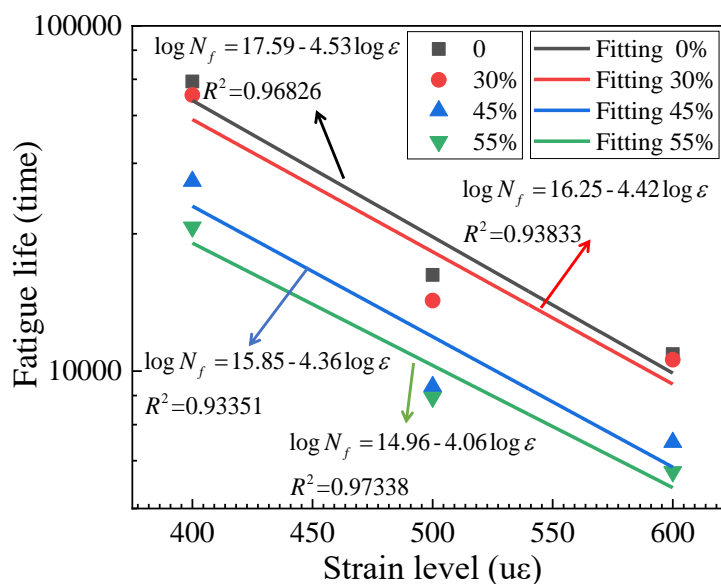


**Figure 6.** Fatigue-strain equation of recycled mixture.

As can be seen from Figure 6, for the four types of mixture, the fatigue life has a high linear correlation with the strain level under the double logarithmic coordinate system, and the correlation coefficients are all greater than 0.93. The loading strain level has a significant effect on the fatigue life of asphalt mixtures. For the mixtures with different RAP contents, the fatigue life decreases significantly with the increase of the strain level. In addition, the slope and intercept of the fatigue-strain equation of the four RAP contents are different, indicating that the RAP content has a certain effect on the fatigue performance of the recycled mixture. As the RAP content increases, the fatigue life and sensitivity to strain of the recycled mixture decreases. The slope and intercept of the mixture with 0% RAP content are the largest, which indicates that the sensitivity between fatigue life and strain level is the largest and the fatigue resistance level is the best. This is due to the existence of aging asphalt in the RAP, which decreases the ability to bear the load, reducing the fatigue life. For the mixture with 30% RAP content, the slope and intercept are not much different from the mixture without old material, indicating that the fatigue life and strain sensitivity and anti-fatigue level between the two are not much different. Similarly, 45 and 55% RAP content mixtures show a similar trend. Overall, with the increase of RAP content, the sensitivity between fatigue life and strain of the mixture gradually decreases, and the anti-fatigue level gradually increases. From the perspective of fatigue life, when the RAP content exceeds 30%, the fatigue life under each strain level shows a tendency to decrease rapidly. Therefore, from the perspective of ensuring the good performance of the mixture, it is more appropriate to control the RAP content within 30%.

#### 4.2. Fatigue performance analysis based on energy analysis

Energy analysis method was used to calculate the fatigue properties of recycled mixtures with different RAP contents, and the results are shown in Figure 7.

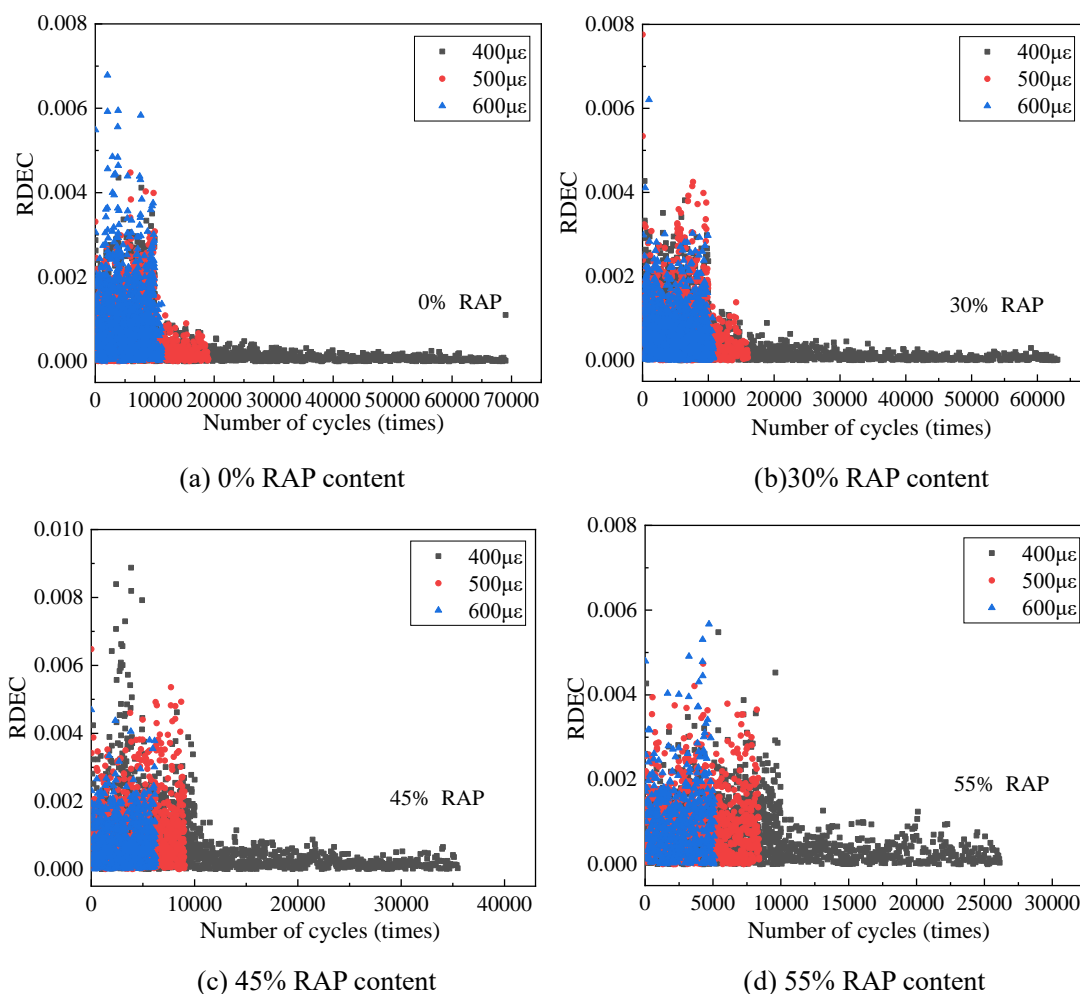


**Figure 7.** Relative change rate of dissipated energy of recycled mixtures.

As can be seen from Figure 7, the RDEC of recycled asphalt mixture presents a similar two-stage change rule with the increase of the number of cycles. At the beginning of the first stage when the cyclic load is applied, the regenerated specimen will undergo structural changes in response to the action of the external load. At this time, more dissipated energy is required and the RDEC is large, but the overall trend is decreasing because the generation of initial crack requires more energy consumption. With the accumulation of energy in the loading process, the internal damage of materials accumulates. At this time, further loading will reduce the RDEC, which also proves that in the fatigue damage process of materials, the initial energy consumption accounts for the majority of the total process. The second stage shows that with the continuous increase of cyclic load, the RDEC decreases somewhat compared with the first stage and exists at a relatively stable state value. This indicates that the asphalt mixture responds to the load with stable energy change, that is, the regenerated specimens undergo fatigue evolution at a stable damage rate, and the variation law of RDEC becomes less obvious with the increase of strain level. In the relevant study [31], the test termination condition was set as the stiffness modulus decreased to 30% of the initial stiffness modulus, and the trend of RDEC would appear the third stage. With the increase of the number of cycles, RDEC would increase, that is, fatigue failure of the specimen would produce cracks, and the damage speed would accelerate. In this test, the test was stopped when the stiffness modulus dropped to 50% of the initial stiffness modulus, so the

third stage did not occur, meaning that the material could still provide energy under the load and was not destroyed. As can be seen from Figure 7, the RDEC of the recycled mixture under different RAP contents and strain levels shows different change rules. The higher the RAP content, the higher the strain level, the less obvious the RDEC, the less likely the second stage phenomenon is to appear, and the fewer the corresponding test termination cycles, which is consistent with the test results in Section 4.1.

In addition, it can be seen from Figure 7 that the stable values of the RDEC in the second stage of various asphalt mixtures under different strains show different rules, and the corresponding stable values also show an increasing trend with the increase of strains. Therefore, the plateau value (PV) of the RDEC in the second stage region can be calculated as an analytical index to study the stable value of the change rate of dissipated energy of different reclaimed asphalt mixtures. Taking PV as the research parameter, the equation between PV and fatigue life is shown in Eq (13).

$$PV = aN_f^b \quad (13)$$

where  $a$  and  $b$  are fitting parameters and fatigue life respectively.

Taking recycled asphalt mixture with 0% RAP content as an example, the specific calculation of the PV in the second stage is described, as shown in Figure 8.

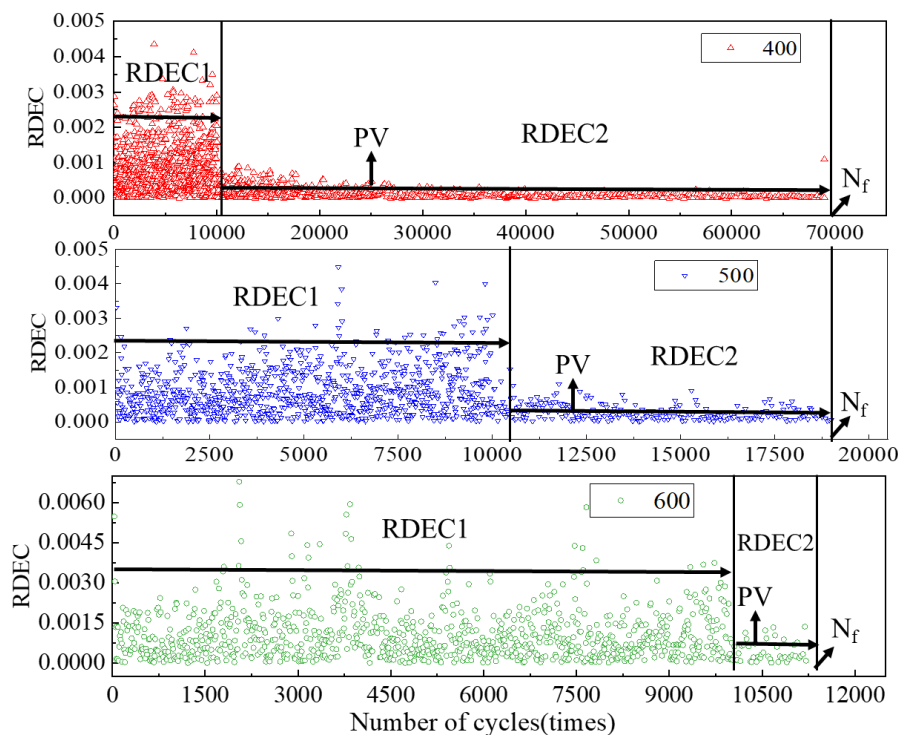


**Figure 8.** PV calculation diagram of recycled mixture.

It can be proved again in Figure 8 that the RDEC of a recycled asphalt mixture presents a similar two-stage change rule with the increase of the number of cycles. In the first stage, the overall RDEC value is large, indicating that fatigue accumulation occurs under the initial load with a large relative change rate of dissipated energy. In the second stage, with the increase of the number of cycles, RDEC

decreases somewhat compared with the first stage and exists in a relatively stable state value. The change law of the second stage is more clearly shown in the figure. Therefore, the calculation of PV in the second stage area can be used as an indicator of fatigue performance of the mixture. Initially, the dividing point of asphalt mixture with RAP content in two stages was found, and then the PV of each mixture under different strains in the second stage was obtained. The calculation results are shown in Table 8.

**Table 8.** PV and fatigue life of recycled asphalt mixture.

RAP content	Strain level ( $\mu\varepsilon$ )	PV	Fatigue life (times)
0%	400	1.45E-04	69,010
	500	2.99E-04	19,000
	600	6.89E-04	11,200
30%	400	1.72E-04	63,050
	500	3.56E-04	16,010
	600	3.4E-04	10,790
45%	400	2.87E-04	35,480
	500	8.91E-04	9030
	600	11.36E-04	6220
55%	400	3.16E-04	26,130
	500	9.72E-04	8400
	600	10.06E-04	5110

It can be seen from Table 8 that for the same asphalt mixture, with the increase of strain level, the PV shows an increasing trend. The greater the strain, the faster the damage rate and the faster the strength decline. Under the same strain level, with the increase of RAP content, the fatigue life decreases, and PV increases. The change of PV or fatigue life indicates that the addition of RAP reduces the fatigue performance of recycled asphalt mixtures, and the higher the dosage, the more obvious the reduction level. This is mainly because the viscosity of the aging asphalt in the RAP is lower than that of the new asphalt, which leads to the decrease of the elastic property of the asphalt mixture. In the process of fatigue loading, more dissipated energy needs to be consumed to cope with the damage, and the greater the dosage of the RAP, the more obvious this process is.

It can be seen from the analysis that in addition to the influence of the dosage of RAP on the fatigue performance of the recycled mixture, the strain level also has a significant influence on it. The fatigue performance of the mixture can be evaluated and analyzed by using the change rate of dissipated energy. Based on the data in Table 7, the fatigue life equation of the mixture was studied. Logarithms were taken from both sides of Eq (13), and the following results were obtained:

$$\log PV = \log a + b \log N_f \quad (14)$$

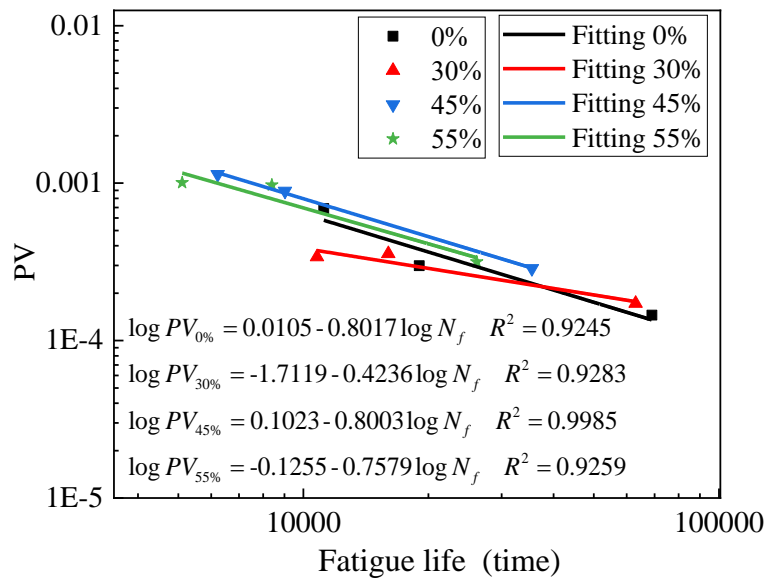


**Figure 9.**  $PV-N_f$  relation equation of recycle mixture.

As can be seen from Figure 9, there is a good linear correlation between  $PV$  in the second stage and fatigue life under the double logarithm coordinates. The correlation coefficients of recycled mixture with different RAP content are 0.9245, 0.9283, 0.9985 and 0.9259, respectively. The results show that it is reasonable to analyze the fatigue damage from the energy point of view and reduce the stiffness modulus to 50% of the initial value as the test termination condition. With the increase of RAP content, the fatigue life tends to decrease. Except for the mixture with 55% RAP content, the slope of the fitted straight line is significantly different from that of other old mixtures due to the influence of the  $PV$  value at high strain levels, and the relationship between  $RDEC-N_f$  of other mixtures is not much different. It is again verified that the  $PV$  in the stable stage can be used to evaluate the fatigue performance of the regenerated mixture, and the analysis is basically consistent with the results in Table 8.

### 4.3. Fatigue damage analysis based on indoor fatigue test

#### 4.3.1. The influence of different strain levels on fatigue damage

Fatigue damage was calculated according to the indoor fatigue test data, and the influence of different strain levels on fatigue damage was analyzed. The calculation and analysis results are shown in Figure 10.



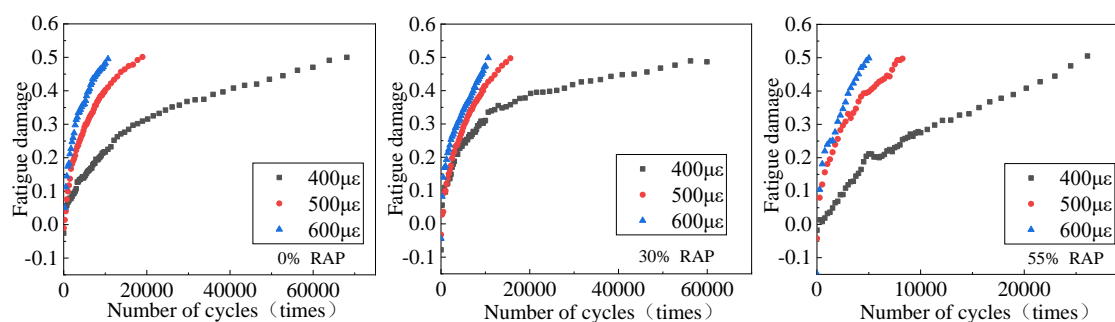


**Figure 10.** Fatigue damage of recycled asphalt mixtures with different RAP contents.

As can be seen from Figure 10, the fatigue damage of all types of mixture shows the same law with the increase of the number of cycles. Fatigue damage increases rapidly at first, and then increases and slows down until the cumulative fatigue damage reaches 50%, which is basically consistent with the two-stage variation law of fatigue parameters analyzed above. At the initial stage, the damage rate increases rapidly due to the action of load. Under the action of load, the microscopic defects inside the structure gradually expand due to stress concentration, resulting in a rapid increase in the amount of specimen damage. With the increase of the number of cycles, the stress concentration inside the defect gradually transfers through the expansion of the defect, resulting in a gradual decrease in the damage rate, and tends to be stable with the load. Then, the material gradually enters the slow damage stage. Under different strain levels, mixtures with the same RAP content different numbers of cycles to reach the final fatigue damage. The greater the strain level, the fewer cycles required and the higher the fatigue damage rate. The cumulative degree of fatigue damage increases with the increase of strain level, and the corresponding fatigue life decreases with the increase of strain level. At the end of the first stage, it can be seen that the strain level has a great influence on the speed of damage accumulation. With the continuous increase of the strain level, the expansion of the microscopic defects in the mixture due to stress concentration becomes more significant, resulting in increased local damage degree, and thus increasing the cumulative damage amount at the end of the first stage. Strain level has relatively little effect on the damage accumulation rate of the second stage, but the fatigue life decreases with the increase of strain level due to the difference of cumulative damage amount at the end of the first stage. In the second stage, the internal damage rate of the material gradually decreases, and the fatigue damage curve gradually slows down. The strain level represents the magnitude of the traffic load. It can be seen that greater traffic load leads to more serious fatigue damage and reduces the fatigue life of asphalt pavement.

In addition, it can also be seen from the figure that the cumulative fatigue damage of each mixture finally reaches 50%, which is caused by the test termination condition reaching 50% of the initial stiffness modulus. By observing the specimen after the fatigue test, it can be found that no macroscopic cracks can be seen on the surface of the specimen at this time, indicating that the specimen has not been broken and still has a certain strength and bearing level. This is consistent with the variation law of cumulative dissipated energy and the results of fatigue damage analysis by dissipated energy theory, and it also proves that the termination conditions of the test are relatively conservative and safe.

#### 4.3.2. The influence of different RAP contents on fatigue damage

Fatigue damage of recycled mixtures with different RAP contents under different strain levels was analyzed, and the analysis results are shown in Figure 11.

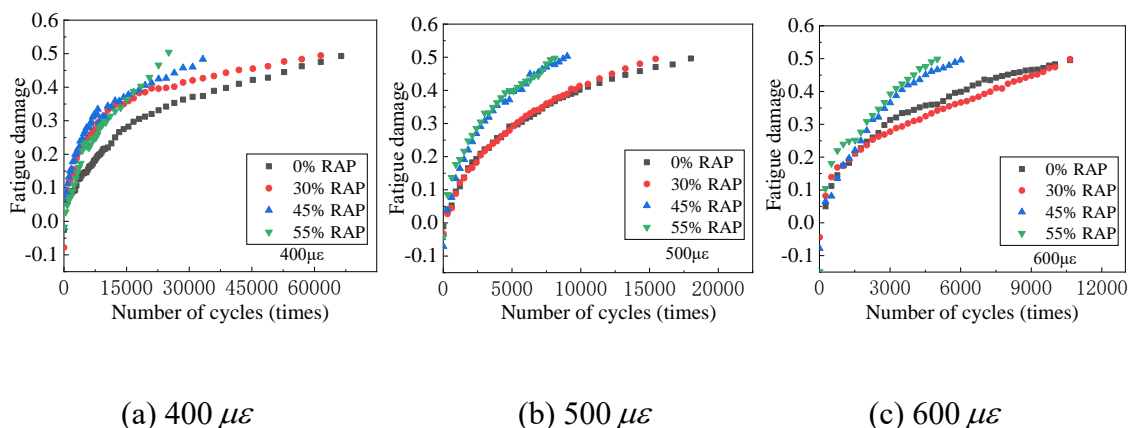


**Figure 11.** Fatigue damage of reclaimed asphalt mixtures under different strains.

As can be seen from Figure 11, under the same strain level, the recycled mixtures with different RAP contents show the same rule of fatigue damage with the increase of the number of cycles. Fatigue damage increases rapidly at first, and then the increase trend slows down until the cumulative fatigue damage reaches 50%. For regenerated mixtures with different RAP contents, the rapid development of fatigue damage is mainly concentrated under the first 25% cyclic load, that is, the fatigue damage mainly occurs in the first stage. With the increase of RAP content, the number of cycles of cumulative fatigue damage reaching 50% at each strain level gradually decreases. Under the same strain level and cycle times, the greater the RAP content, the more obvious the fatigue damage degree. At 400  $\mu\epsilon$  level, the fatigue damage degree of the mixture increases gradually with the RAP content. At the levels of 500 and 600  $\mu\epsilon$ , 0 and 30% RAP content mixtures show similar fatigue damage law. When RAP exceeds 30%, the fatigue damage degree of recycled mixture is intensified. The fatigue damage law of the mixture with 45 and 55% content is basically consistent. This is mainly due to the presence of aged asphalt in RAP, which increases the stiffness of the mixture. With the increase of RAP content, the proportion of aged asphalt in the mixture increases, and the proportion of new asphalt correspondingly decreases, and the two kinds of asphalt cannot be completely fused. The fatigue life of asphalt mixture mainly depends on its own stress relaxation properties and flexibility. When the load changes, the fatigue properties of the aged asphalt are reduced and fatigue micro-cracks are more likely to occur because the self-healing properties, stress relaxation properties, and flexibility of the aged asphalt are worse than those of the new asphalt. In addition, the existence of new and old aggregates causes the segregation of the mixture, and the uniformity of the mixture decreases with the increase of RAP content, which also has an adverse effect on fatigue damage. Therefore, from the aspect of fatigue damage, the proportion of recycled aggregate should be controlled.

#### 4.4. Fatigue damage field distribution based on finite element analysis

##### 4.4.1. Fatigue damage field of recycled mixture at different temperatures

In the numerical simulation of fatigue damage of recycled asphalt mixture, the tensile stress at the center of the bottom surface of the trabecular specimen was obtained first. According to the mesh division of the finite element model, the damage distribution of all trabecular specimen elements can be calculated and the fatigue damage behavior of the recycled mixture can be analyzed. In order to simplify the calculation, the fatigue damage analysis of the regenerated specimen with 45% RAP content was carried out in the finite element model. The influence of different temperature conditions on the fatigue damage performance of the recycled mixture was analyzed. The variation of tensile stress on the bottom surface of the trabecular specimen with various temperatures is shown in Figure 12.

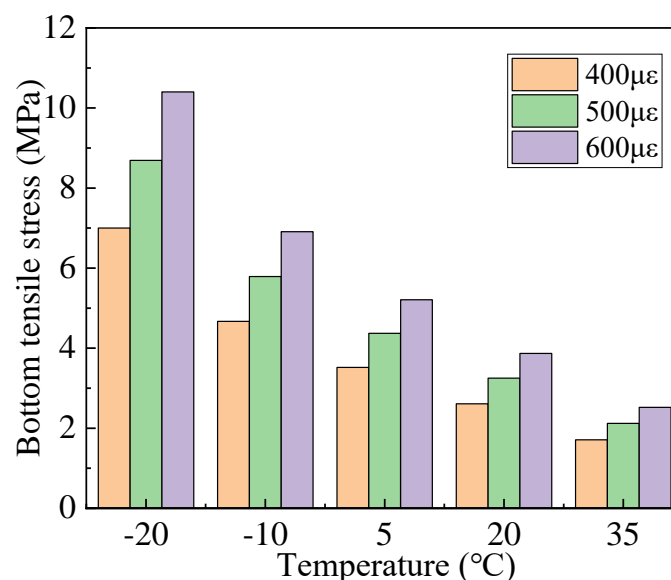


**Figure 12.** Variation of bottom tensile stress with temperatures.

As can be seen from Figure 12, under the same strain level, the tensile stress at the bottom of the recycled asphalt mixture beam with the same RAP content shows a gradually decreasing trend with the increase of temperature. This is mainly because with the increase of temperature, the elastic property of asphalt decreases, the cohesive force decreases, the viscosity of the mixture increases, and the dynamic modulus decreases. At the same strain level, the modulus decreases gradually with the increase of temperature, so the stress also shows the trend of decreasing gradually.

The fatigue damage distribution of recycled mixtures under the same fatigue frequency at different temperatures was simulated. Due to the large number of numerical simulation cloud images, the three-dimensional damage diagram of the trabeculae as a whole takes  $-20^{\circ}\text{C}$  as an example, and the internal damage field of regenerated specimens at different temperatures is shown in Figure 13.

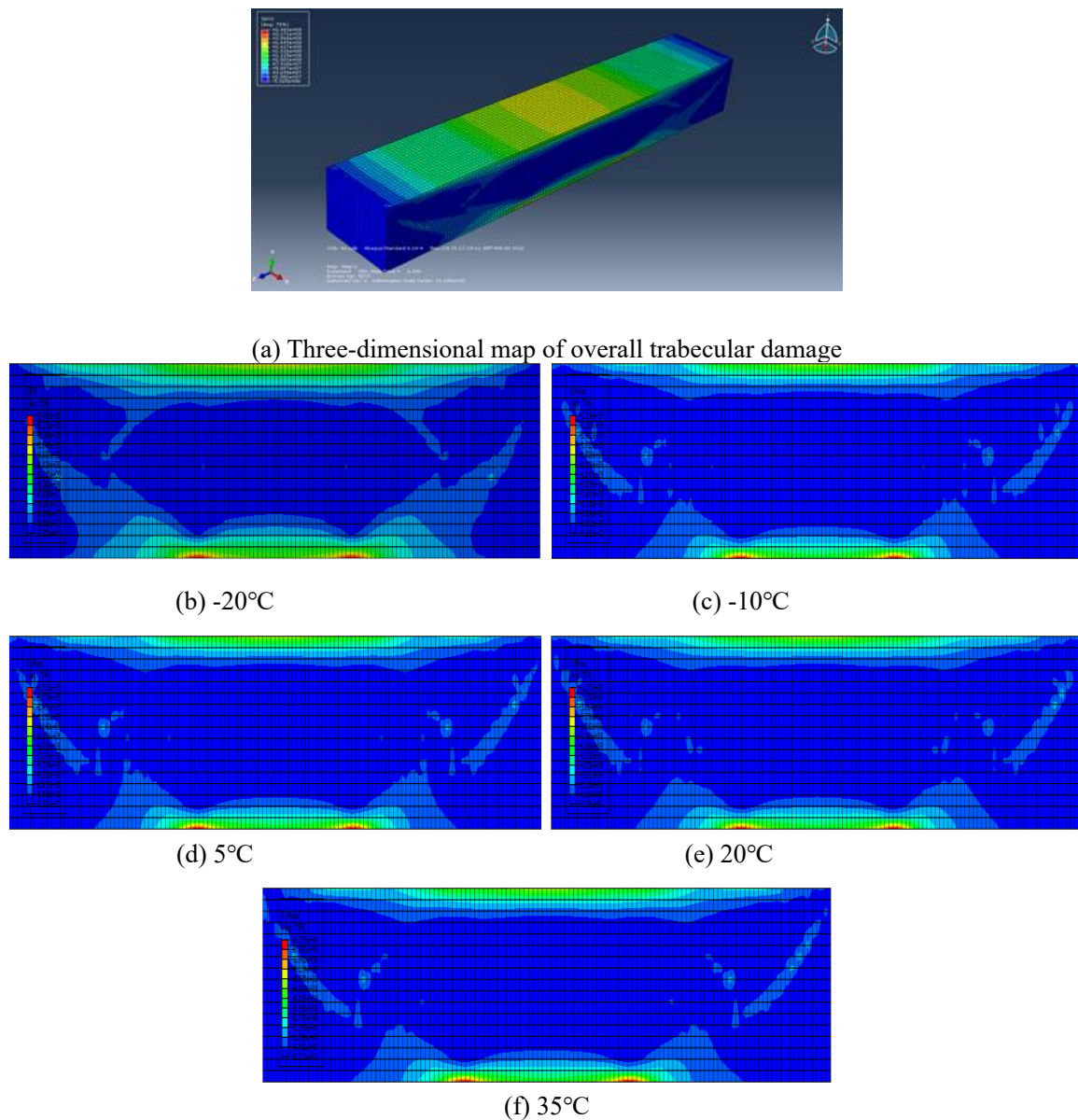


**Figure 13.** Trabecular fatigue damage field distribution cloud map with the same fatigue action at different temperatures.

As can be seen from Figure 13, the overall damage of trabecular specimens can be characterized by finite element numerical simulation. The overall damage of the specimen is mainly generated between two jigs in the middle of the trabecular, and the middle of the trabecular was basically in a state of pure bending structure. The overall damage is mainly generated at the parts of the specimen bearing compressive stress at the upper part and tensile stress at the bottom, and the damage field distribution area accounts for a small part of the overall specimen area. The stress concentration phenomenon under the middle two clamps is obvious, and the resulting damage field is the largest. It is expected that the initial crack will be generated near or in between the two points. With the gradual increase of temperature, the damage field distribution at the bottom of trabecular specimen shows a trend of decreasing under the same cyclic fatigue load. This is mainly caused by the viscoelasticity of the material, which largely determines the stress response and fatigue failure of the pavement structure.

Due to the increase of temperature, the asphalt elasticity decreases, the adhesive force decreases, the viscosity of the mixture increases (which is manifested as the decrease of modulus) and the lower bottom tensile stress decreases for the same load times. This indicates that under the condition of low temperature, the fatigue property of the mixture becomes worse, the fatigue damage accumulation speed becomes faster, and the fatigue crack generation speed will be accelerated. In the actual pavement service environment, attention should be paid to the fatigue performance of the recycled mixture at low temperatures. Revealing the fatigue damage mechanism of recycled asphalt mixtures from the perspective of the overall damage field has important theoretical significance for analyzing the low temperature fatigue failure of recycled asphalt mixtures caused by stress concentration and also for the timely determination of the maintenance opportunities of each stage.

#### 4.4.2. Fatigue damage field of recycled mixture at different strain levels

The influence of different strains on fatigue damage properties of recycled mixture was obtained by analyzing Figure 12. The tensile stress at the bottom of the recycled asphalt mixture trabecular increases with the increase of strain level at each temperature. The main reason is that the larger the strain level, the larger the microdeformation of the specimen during loading, the more serious the internal damage of the specimen, the greater the speed of microcrack initiation and development, and the greater the tensile stress of the beam bottom. Taking the temperature of 20 °C as an example, the fatigue damage distribution of the recycled mixture under the same fatigue load and different strains was simulated. The internal damage field distribution of the regenerated specimen under different strains is shown in Figure 14.

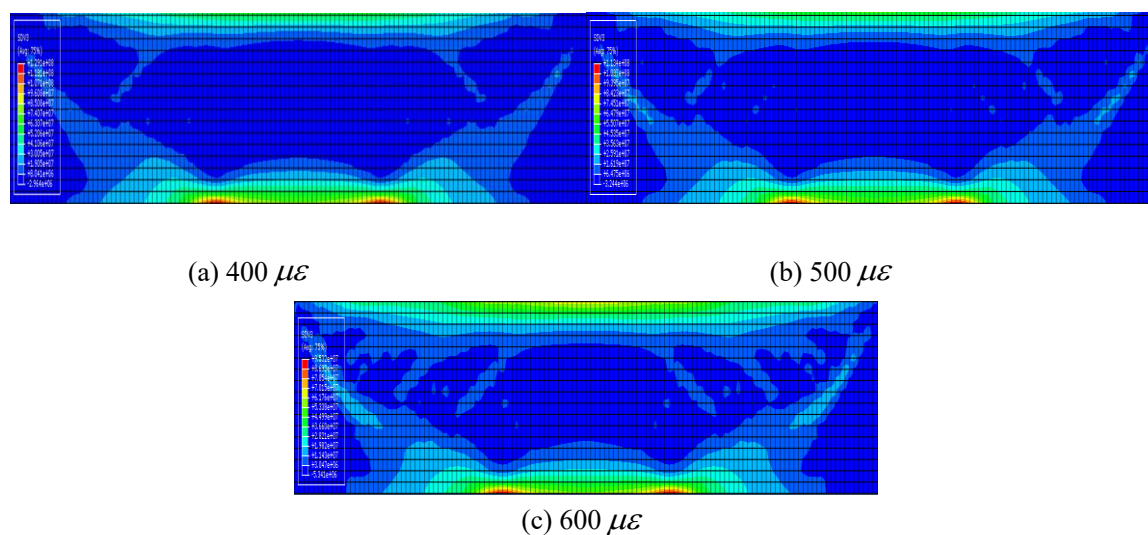


**Figure 14.** Distribution nephogram of trabecular fatigue damage field under different strains.

As can be seen from Figure 14, under the same fatigue load, the maximum damage of the mixture and the distribution of damage field in the beam increase as the strain increases. The overall damage of trabecular specimen is mainly distributed near the middle two clamps and the middle part. In the damage distribution at the bottom of the side beam, the damage field distribution shows that the two sides are larger than the middle “saddle shape” distribution, and the damage is the largest at the bottom

corresponding to the loading point. With the action of continuous loading, the initial crack will be generated near or in between the two loading points, which is also consistent with the actual laboratory test results. The damage distribution is uneven in the lateral direction. With the action of load, the damage will accumulate continuously, and the non-uniformity will be gradually amplified. Under different strains, the damage distribution range also has obvious differences, which also reflects that damage accumulation is highly sensitive to strain level.

#### 4.4.3. Fatigue damage field of recycled mixtures with different RAP contents

The temperature was set at 20°C and the strain level was set at 500  $\mu\epsilon$ . The effect of different RAP contents on the fatigue damage properties of the recycled mixtures was analyzed, and the results are shown in Figure 15.

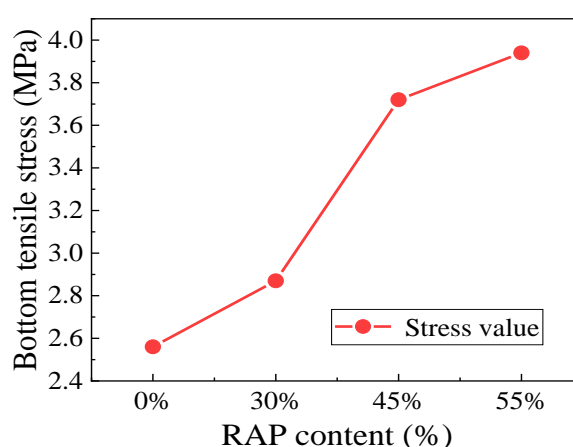


**Figure 15.** Variation of bottom tensile stress of different regenerated specimens.

It can be seen from Figure 15 that under the same fatigue load, the tensile stress at the bottom of the recycled asphalt mixture beam gradually increases with the increase of RAP content. The 0% RAP content mixture displays the smallest beam bottom stress level, and the 30, 45 and 55% RAP content specimens show beam bottom stress level increases of 12, 40 and 50% respectively when compared to the 0% RAP specimen. This is mainly because the increase of RAP content will increase the percentage of aging asphalt in the mixture. After aging, the viscosity and penetration degree of asphalt will change and the elasticity will increase, resulting in the increase of dynamic modulus, so that the tensile stress of the bottom surface of the specimen will increase under the same fatigue action. From the point of view of the tensile stress level under fatigue load, the regenerated mixture with less than 45% RAP content has better performance. Under the action of the same strain level and fatigue frequency, the fatigue damage distribution of the recycled mixture with different RAP content was simulated, and the internal damage field of the regenerated specimen is shown in Figure 16.

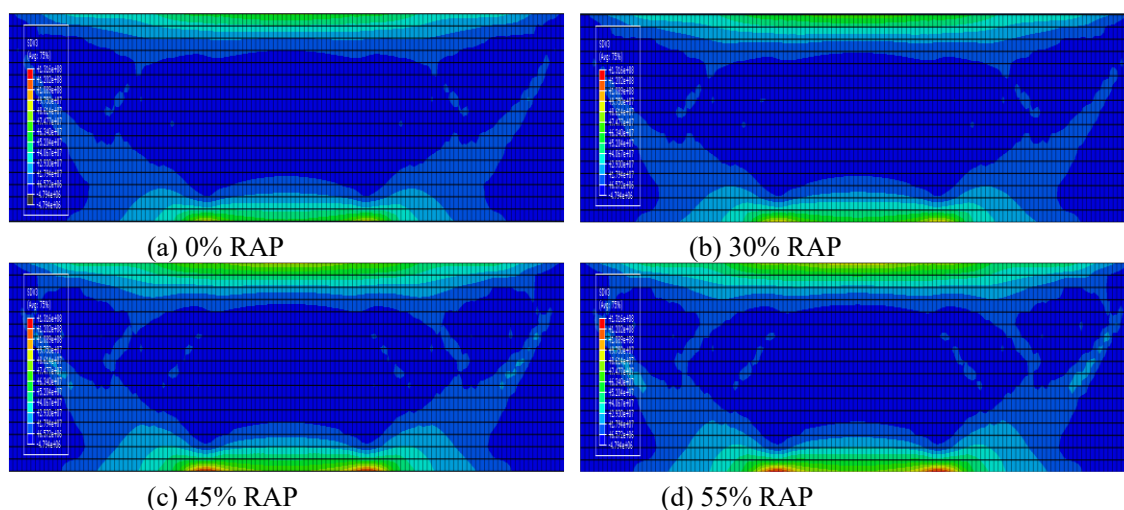


**Figure 16.** Fatigue damage field distribution of trabecular regenerated mixture with different RAP content.

The damage field distribution of different types of recycled mixtures also shows the “saddle-shaped” distribution characteristic where two sides are larger than the middle and the damage is the largest at the bottom corresponding to the loading point. As can be seen from Figure 16, under the same fatigue load, with the increase of RAP content, the fatigue damage distribution area of trabecular specimens slightly increases, and shows an increasing trend of gradual upward expansion. The damage field of the trabecular specimens with 0 and 30% RAP content has little difference, and the damage field distribution range of the specimens with 55% RAP content is obviously the largest. It shows that with the increase of RAP content, the proportion of aging asphalt in the recycled mixture also increases and the new asphalt and old asphalt cannot be completely integrated, resulting in the decline of fatigue performance of the recycled asphalt mixture. The higher the RAP content, the more obvious the phenomenon will be. Therefore, from the aspect of fatigue damage, the proportion of RAP should be controlled.

## 5. Conclusions

In this paper, four point bending fatigue tests and finite element numerical simulations were used to analyze the fatigue properties and fatigue damage of recycled mixtures with different RAP contents. The main conclusions are as follows:

1) The fatigue prediction equation based on phenomenological method was established, and the fatigue property variation rule of recycled mixtures with different RAP contents was analyzed. With the increase of RAP content, the fatigue life of the mixture decreased gradually and the sensitivity of fatigue life to strain decreased gradually.

2) Based on the dissipated energy theory, the ratio of dissipated energy change was proposed as an important index to evaluate the fatigue performance of recycled asphalt mixtures. The two-stage change law of the relative change rate of dissipated energy was obtained as the number of load cycles increased. By establishing the correlation between the plateau value and the fatigue life under the double logarithm coordinates, the influence law of used material content on the fatigue performance of recycled mixtures was analyzed, which provided a theoretical basis for determining the reasonable

content of recycled mixtures.

3) Based on the damage mechanics theory, stiffness modulus was proposed to characterize the fatigue damage of recycled asphalt mixtures. The fatigue damage change rate of recycled asphalt mixture under different RAP contents and strain levels was comprehensively evaluated, and the fatigue damage evolution process of recycled asphalt mixtures with different RAP contents under load was analyzed.

4) The finite element numerical model of fatigue damage of recycled asphalt mixtures was established. The distribution and variation of bottom stress and internal damage field of trabecular specimens under different temperatures, strain levels and RAP contents were systematically studied. For future work, establishing the possible correlation between fatigue tests and simulation results would enrich the work done in this study.

### Use of AI tools declaration

The authors declare that they have not used Artificial Intelligence (AI) tools in the creation of this article.

### Acknowledgments

This work was supported by the “Key Laboratory for Special Area Highway Engineering of Ministry of Education, Chang’an University” (300102213506), “Xizang Natural Science Foundation” (XZ2018ZRG-69). Thanks to all those who have provided guidance and assistance for this article.

### Conflict of interest

The authors declare no conflict of interest.

### References

1. L. Gu, *Meso-Simulation Study on Pavement Performance of Asphalt Mixture Based on Viscoelastic Damage and Fracture Mechanics*, Southeast University, 2019.
2. F. N. Hveem, Pavement fatigue deflections and fatigue failures, *Highw. Res. Board, Bull.*, **1** (1955), 43–87.
3. P. Pell, Characterization of fatigue behavior, *Highw. Res. Board, Spec. Rep.*, **49** (1973), 49–64.
4. C. Monismith, J. Epps, F. Finn, Improved asphalt mix design (with discussion), *Assoc. Asphalt Paving Technol. Proc.*, **54** (1985), 347–406.
5. S. Lv, J. Zheng, *Normalization Method for Asphalt Mixture Fatigue Equation Under Different Loading Frequencies*, *Journal of Central South University*, **22** (2015), 2761–2767. <https://doi.org/10.1007/s11771-015-2806-1>
6. S. Lv, J. Zheng, Fatigue properties of asphalt mixtures under broad stress ratio conditions: Improved S-N model, *J. Highw. Transp. Res. Dev.*, **7** (2011), 1–6. <https://doi.org/10.1061/JHTRCQ.0000019>



7. D. Ge, Z. Ju, D. Duan, S. Lyu, W. Lu, C. Liu, Normalized fatigue properties of asphalt mixture at various temperatures, *J. Road Eng.*, **3** (2023), 279–287. <https://doi.org/10.1016/j.jreng.2023.05.001>
8. N. Sudarsanan, Y. R. Kim, A critical review of the fatigue life prediction of asphalt mixtures and pavements, *J. Traffic Transp. Eng.*, **9** (2022), 808–835. <https://doi.org/10.1016/j.jtte.2022.05.003>
9. N. Tapsoba, C. Sauzéat, H. Di Benedetto, H. Baaj, M. Ech, Behaviour of asphalt mixtures containing reclaimed asphalt pavement and asphalt shingle, *Road Mater. Pavement*, **15** (2014), 330–347. <https://doi.org/10.1080/14680629.2013.871091>
10. W. S. Mogawer, E. H. Fini, A. J. Austerman, A. Booshehrian, B. Zada, Performance characteristics of high reclaimed asphalt pavement containing bio-modifier, *Road Mater. Pavement*, **17** (2016), 753–767. <https://doi.org/10.1080/14680629.2015.1096820>
11. B. Visintine, N. P. Khosla, A. Tayebali, Effects of higher percentage of recycled asphalt pavement on pavement performance, *Road Mater. Pavement*, **14** (2013), 432–437. <https://doi.org/10.1080/14680629.2013.779310>
12. A. Kavussi, A. Modarres, Laboratory fatigue models for recycled mixes with bitumen emulsion and cement, *Constr. Build. Mater.*, **24** (2010), 1920–1927. <https://doi.org/10.1016/j.conbuildmat.2010.04.009>
13. S. L. Schuster, C. Faccin, F. D. Boeira, L. P. Specht, D. D. Pereira, L. A. H. do Nascimento, Fatigue behaviour of plant produced asphalt mixtures through viscoelastic continuum damage model, *Road Mater. Pavement*, **24** (2023), 59–85. <https://doi.org/10.3141/2506-04>
14. T. Ma, X. Ding, D. Zhang, X. Huang, J. Chen, Experimental study of recycled asphalt concrete modified by high-modulus agent, *Constr. Build. Mater.*, **128** (2016), 128–135. <https://doi.org/10.1016/j.conbuildmat.2016.10.078>
15. Y. Gao, D. Geng, X. Huang, G. Li, Degradation evaluation index of asphalt pavement based on mechanical performance of asphalt mixture, *Constr. Build. Mater.*, **140** (2017), 75–81. <https://doi.org/10.1016/j.conbuildmat.2017.02.095>
16. N. Guo, Z. You, Y. Zhao, Y. Tan, Durability of warm mix asphalt containing recycled asphalt mixtures, *China J. Highw. Transp.*, **27** (2014), 17–22. <https://doi.org/10.19721/j.cnki.1001-7372.2014.08.003> (in Chinese)
17. Z. He, L. Chen, X. Chen, Y. Cheng, Mechanical properties and application research of hot recycled asphalt mixture from central mixing plant, *J. Build. Mater.*, **19** (2016), 871–875. <https://doi.org/10.3969/j.issn.1007-9629.2016.05.015>
18. Z. Wang, L. Cai, X. Wang, C. Xu, B. Yang, J. Xiao, Fatigue performance of different thickness structure combinations of hot mix asphalt and cement emulsified asphalt mixtures, *Materials*, **11** (2018). <https://doi.org/10.3390/ma11071145>
19. S. Noura, E. Yaghoubi, S. Fragomeni, P. L. P. Wasantha, R. Van Staden, Fatigue and stiffness characteristics of asphalt mixtures made of recycled aggregates, *Int. J. Fatigue*, **174** (2023). <https://doi.org/10.1016/j.ijfatigue.2023.107714>
20. K. Sapkota, E. Yaghoubi, P. L. P. Wasantha, R. Van Staden, S. Fragomeni, Mechanical characteristics and durability of HMA made of recycled aggregates, *Sustainability*, **15** (2023). <https://doi.org/10.3390/su15065594>
21. Ministry of Transport, Technical specifications for construction of highway asphalt pavements (JTG F40-2004), *People's Communications Press*, 2004.

22. Ministry of Transport, Test methods of aggregate for highway engineering (JTG E42-2005), *People's Communications Press*, 2005.
23. Ministry of Transport, Standard test methods of bitumen and bituminous mixtures for highway Engineering (JTG E20-2011), *People's Communications Press*, 2011.
24. Ministry of Transport, Technical specifications for highway asphalt pavement recycling (JTG/T 5521-2019), *People's Communications Press*, 2019.
25. X. Cai, J. Yang, *A Fatigue Damage Model for Asphalt Mixtures Under Controlled-Stress and Controlled-Strain Mode*, *Journal of Southeast University (English Edition)*, **35** (2019), 89–96. <https://doi.org/10.3969/j.issn.1003-7985.2019.01.013>
26. J. Zhang, Z. Li, *Viscoelastic Plastic Damage Constitutive Model of Asphalt Mixture Under Cyclic Loading*, *Journal of Northeastern University (Natural Science Edition)*, **40** (2019), 1496–1503. <https://doi.org/10.12068/j.issn.1005-3026.2019.10.023>
27. H. J. Lee, J. S. Daniel, Y. R. Kim, Continuum damage mechanics-based fatigue model of asphalt concrete, *J. Mater. Civil Eng.*, **12** (2000), 105–112. [https://doi.org/10.1061/\(ASCE\)0899-1561\(2000\)12:2\(105\)](https://doi.org/10.1061/(ASCE)0899-1561(2000)12:2(105))
28. W. Huang, X. Deng, A new fatigue response model of asphalt mixture, *China J. Highw. Transp.*, **1** (1995), 56–62
29. L. Wang, L. Wang, L. Feng, F. Zhang, Fatigue properties of warm-mix crumb rubber modified asphalt mixture, *J. Build. Mater.*, **21** (2018), 497–502. <https://doi.org/10.3969/j.issn.1007-9629.2018.03.024>
30. S. H. Shen, S. H. Carpenter, Application of the dissipated energy concept in fatigue endurance limit testing, *Transp. Res. Rec.*, (2005), 165–173. <https://doi.org/10.3141/1929-20>
31. H. Guan, J. Zheng, X. Tian, Comparing of Fatigue Damage Defining Ways of Asphalt Mixtures, in *International Conference on Transportation Engineering*, 2009. [https://doi.org/10.1061/41039\(345\)453](https://doi.org/10.1061/41039(345)453)
32. Y. R. Kim, H. J. Lee, D. N. Little, Fatigue characterization of asphalt concrete using viscoelasticity and continuum damage theory (with discussion), *J. Assoc. Asphalt Paving Technol.*, **66** (1997). <http://worldcat.org/issn/02702932>
33. F. Zhang, *Research on Pavement Performance of Asphalt Mixture modified by Warm Mixed rubber Powder*, Inner Mongolia University of Technology, 2018.
34. A. Wu, *Research on Evaluation Method of Fatigue Resistance of Asphalt Mixture*, Southeast University, 2016.
35. H. Zhang, J. Zhao, *Application of Fatigue Damage Mechanics to Metal Components*, Beijing: National Defense Industry Press, 1998.



AIMS Press

©2024 the Author(s), licensee AIMS Press. This is an open access article distributed under the terms of the Creative Commons Attribution License (<http://creativecommons.org/licenses/by/4.0>)